MTMO grayscale photomask

Chuan Fei Guo[1,2], Jianming Zhang[1,2] Junjie Miao[1,3] Yongtao Fan[4] and Qian Liu[1,*]

[1]*National Center for Nanoscience and Technology, No. 11, Beiyitiao, Beijing 100190, China*
[2]*Graduate School of the Chinese Academy of Sciences, Beijing 100080, China*
[3] *Academy for Advanced Interdisciplinary Studies, Beijing Uviversity, Zhongguancun, Beijing 100871, China*
[4]*Shanghai Institute of Optics and Fine Mechanics, Chinese Academy of Sciences, No. 390, Qinghe Road, Shanghai*
liuq@nanoctr.cn

Abstract: We present a new class of simple, cheap and stable grayscale photomasks based on the metal-transparent-metallic-oxides (MTMO) systems by laser direct writing in metal films. For obtaining high resolution and grainless grayscale patterns we developed a refinement method of the films, in which the nanometer size effect may play a significant role for the improvement. We propose a layered oxidation model and a grain model for the mechanism of In- and Sn-based MTMO systems. The masks have a wide application wavelength range at least from 350 to 700 nm. Three-dimensional microstructures have been successfully fabricated by using the MTMO grayscale masks.

OCIS codes: (160.4236) Nanomaterials; (310.6845) Thin film devices and applications; (110.6895) Three-dimensional lithography; (160.3900) Metals.

References and links

1. J. D. Rogers, A. H. O. Kärkkäinen, T. Tkaczyk, J. T. Rantala, and M. R. Descour, "Realization of refractive microoptics through grayscale lithographic patterning of photosensitive hybrid glass," Opt. Express **12**(7), 1294–1303 (2004).
2. K. Reimer, H. J. Quenzer, M. Jürss, and B. Wagner, "Micro-optic fabrication using one-level gray-tone lithography," Proc. SPIE **3008**, 279–288 (1997), http://www.mp-cc.de/docs/reiphot.pdf.
3. M. Christophersen, and B. F. Phlips, "Gray-tone lithography using an optical diffuser and a contact aligner," Appl. Phys. Lett. **92**(19), 194102 (2008).
4. C. M. Waits, A. Modafe, and R. Ghodssi, "Investigation of gray-scale technology for large area 3D siliconMEMS structures," J. Micromech. Microeng. **13**(2), 170–177 (2003).
5. C. K. Wu, "Method of making high energy beam sensitive glasses," U.S. Patent, No. 5,078,771 (1992).
6. G. Gal, "Method for fabricating microlenses," U.S. Patent No. 5,310,623, 10, (1994).
7. C. G. Granqvist, and A. Hultaker, "Transparent and conducting ITO films: new developments and applications," Thin Solid Films **411**(1), 1–5 (2002).
8. Z. W. Pan, Z. R. Dai, and Z. L. Wang, "Nanobelts of semiconducting oxides," Science **291**(5510), 1947–1949 (2001).
9. E. Comini, "Metal oxide nano-crystals for gas sensing," Anal. Chim. Acta **568**(1-2), 28–40 (2006).
10. B. Krishnamachari, J. McLean, B. Cooper, and J. Sethna, "Gibbs-Thomson formula for small island sizes: Corrections for high vapor densities," Phys. Rev. B **54**(12), 8899–8907 (1996).
11. E. P. Domashevskaya, O. A. Chuvenkova, V. M. Kashkarov, S. B. Kushev, S. V. Ryabtsev, S. Yu. Turishchev, and Yu. A. Yurakov, "TEM and XANES investigations and optical properties of SnO nanolayers," Surf. Interface Anal. **38**(4), 514–517 (2006).
12. C. K. Wu, "gray scale all-glass photomasks," U.S. Patent No. 2005/0053844 A1, (2005).
13. C. F. Guo, Z. Zhang, S. Cao, and Q. Liu, "Laser direct writing of nanoreliefs in Sn nanofilms," Opt. Lett. **34**(18), 2820–2822 (2009).
14. C. F. Guo, S. Cao, P. Jiang, Y. Fang, J. Zhang, Y. Fan, Y. Wang, W. Xu, Z. Zhao, and Q. Liu, "Grayscale photomask fabricated by laser direct writing in metallic nano-films," Opt. Express **17**(22), 19981–19987 (2009), http://www.opticsinfobase.org/abstract.cfm?URI=oe-17-22-19981.

1. Introduction

The grayscale lithography is an efficient technique for the fabrication of three-dimensional (3D) microstructures in the field of micro-electro-mechanical systems (MEMS) and micro-optics [1–4]. However, the current mainstream techniques for making grayscale masks, i.e., high-energy-beam-sensitive (HEBS) glass and chrome on glass (COG) grayscale mask

#121143 - $15.00 USD Received 8 Dec 2009; revised 12 Jan 2010; accepted 12 Jan 2010; published 25 Jan 2010

[2,5,6], are often too costly for practical applications, thus the creation of a grayscale mask with low cost is of great significance.

The transparent metallic oxides such as In_2O_3 and SnO_2 are star materials in the photo-electrical industry owing to their applications in the field of transparent conductive films, for example, ITO film (tin doped indium oxide) that has been widely used [7]. In recent years, the oxides of In, Sn and Zn are in the spotlight because of the diverse morphologies and desired photo-electrical properties of the In_2O_3, SnO_2 and ZnO nanostructures [8]. These oxides are also good candidates for gas sensors [9]. Here we present a new application of the metals in the field of microfabrication for fabricating novel true grayscale masks based on the metal-transparent-metallic-oxide(s) (MTMO) systems, by using the laser direct writing (LDW) technique. Only two steps are required in the process of the MTMO mask fabrication, *i.e.*, metallic film deposition and laser direct writing in the film. Obviously, the MTMO grayscale masks are simple and inexpensive compared with the HEBS glass that has to use the costly e-beam writer, or a COG grayscale mask that need multi-steps of high-resolution lithography and complicated grayscale calibration. However, fabrication of the MTMO grayscale mask is not an easy task because the as-deposited In or Sn films often have big grains and rough surfaces. Ostwald ripening is the main reason of the low quality of the films, that is, finer grains are unstable and are incorporated into bigger ones via a vapor phase process. Therefore, how to prepare a film with fine grains is a key to get high-resolution masks.

The In_2O_3 or SnO_2 formed in the laser-induced oxidation are very transparent in the visible and near-ultraviolet (NUV) region down to 350 nm, and the transparency of the laser-induced patterned films can be largely tuned from that of the oxide to that of the corresponding metal, that means these grayscale masks are suitable for common photolithography such as I-line lithography. Therefore, in this paper we take In and Sn as the samples to study the fabrication of MTMO grayscale mask with grainless and high-resolution features, based on a special refinement process of the films developed by us. In addition, we also discussed the structure of the MTMO grayscale masks and proposed two models to clarify the mechanism of In and Sn grayscale masks, respectively.

2. Experiments

2.1 Film deposition and laser direct writing

The In and Sn films (10-60 nm) were deposited on glass substrates by radio-frequency magnetron sputtering with a power of 30 W and pressure of 0.57 Pa. The grayscale mask fabrication was performed using a home-built laser direct writer adopted a 532 nm laser (Spectra Physics, Millennia Pro 2i) with a repetition rate of 250 Hz and a scan width of 200 nm, smaller than the focused laser spot size (~350 nm). Pulse widths changed from 30 ns to 1ms and laser powers changed from 1 to 15 mW were controlled by an acousto-optic modulator. A 10-bit bitmap file including all writing parameters and writing path data was generated to control the writing process.

2.2 Characterization

The optical micrographics of the grayscale masks were taken by optical microscopy (Olympus BX-51). Morphology of the films was observed by field emission scanning electron microscopy (FESEM, Hitachi S-4800) and field emission transmission electron microscopy (FETEM, FEI Tecnai G^2 F20). Structure of the films was measured by high-resolution TEM (HRTEM), selected area electron diffraction (SAED) and x-ray diffraction (XRD, Philips X'pert Pro). Ultraviolet-visible (UV-vis) light spectra were measured by a UV-vis-NIR spectrometer (Perkin Elmer Lambda 950). Three-dimensional microstructures were fabricated via I-line lithography (SUSS MicroTec) and were observed by scanning electron microscopy (SEM, Hitachi S-3400N).

#121143 - $15.00 USD Received 8 Dec 2009; revised 12 Jan 2010; accepted 12 Jan 2010; published 25 Jan 2010

3. Results and discussions

3.1 Preparation of ultra-fine grained In and Sn films and the mechanism of the refinement

The In and Sn films prepared by common physical vapor deposition methods have big grains and rough surfaces when the film thickness exceeds 15 nm. The inhomogeneous morphology makes it difficult to obtain high-resolution and grainless grayscale patterns, so that these grayscale masks are incapable of making microstructures with smooth surface. The Ostwald ripening is the main reason of deterioration of the films. In the ripening process, grains with a smaller surface curvature radius have a larger saturation vapor pressure according to the Gibbs-Thomson equation [10]:

$$p(r) = p_0 \cdot \exp\left(\frac{\gamma}{r\rho kT}\right) \quad (1),$$

where p is the vapor pressure between vapour and the grain with a curvature radius of r, p_0 the vapor pressure of a planar surface, γ the edge free energy per unit length of the two dimensional island or grain, ρ the density of the grain and kT the thermal energy. The pressure gradient will lead to mass transfer of metal vapour from the small grains to the big ones. This process will be accelerated as the small grains get even smaller. Therefore, small grains tend to be vanished while big ones are grown even bigger.

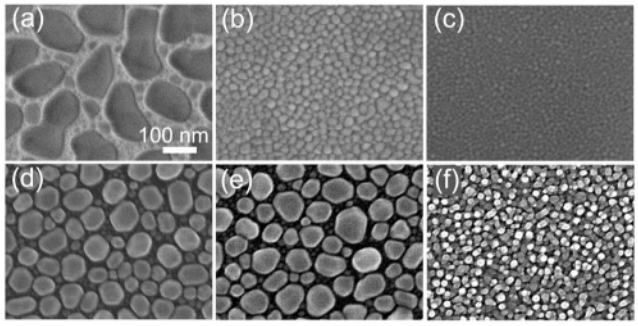

Fig. 1. SEM images of different Sn and In films with the same thickness of 20 nm. (a), (b) and (c) 20 nm Sn films deposited in one time (20 nm), twice (10 nm×2) and four times (5 nm×4), respectively. (d), (e) and (f) 20 nm In film prepared by one time deposition, four times of deposition (film not surface oxidized in the deposition intervals) and four times of deposition (5 nm×4, with surface oxidation for each layer), respectively.

In order to prepare fine grained films, the ripening effect should be suppressed. In other words, suppress the growth of big grains and promote the nucleation process. Here we give a simple method to prepare fine grained and relatively smooth In and Sn films. Our method is consisted of successive deposition of several layers of metallic films with a small thickness (each layer possess ultrafine grains); a coating on every metal layer is introduced to prevent the re-sublimation and growth of the metal grains. Thicker films with fine grains can be obtained by multi-layer deposition. Suppression of the ripping effect was easily realized by exposing the film in the air, or ventilating oxygen in the deposition chamber during the sputtering intervals because an oxide sheath will be formed on the In or Sn grains. For instance, a 20-nm-thick In or Sn film can be obtained by one-off, two-layer or four-layer deposition with a single layer with thickness of 20, 10 and 5 nm, respectively. The latter has the finest grains. As shown in Fig. 1, grain size of the multi-layered films is decreased from the original size of around 100 nm to 10-20 nm. Figure 2 shows the schematic illustration of the routine method and the refinement for preparing Sn or In films. The oxide coating is one or several atomic layer thick so that it does not affect the optical density of the film apparently, while is sufficiently effective in suppressing the ripening effect and increasing the amount of the nuclei, therefore, a remarkable refinement effect is observed.

#121143 - $15.00 USD Received 8 Dec 2009; revised 12 Jan 2010; accepted 12 Jan 2010; published 25 Jan 2010

It should be noted that the deposition interval is not the reason of the refinement, which does not happen if films are not exposed to oxygen ambience in the deposition intervals. The grain size does not change after four times of deposition without surface oxidation (Fig. 1(e)) unless the film was exposed to air in every deposition intervals (Fig. 1(f)).

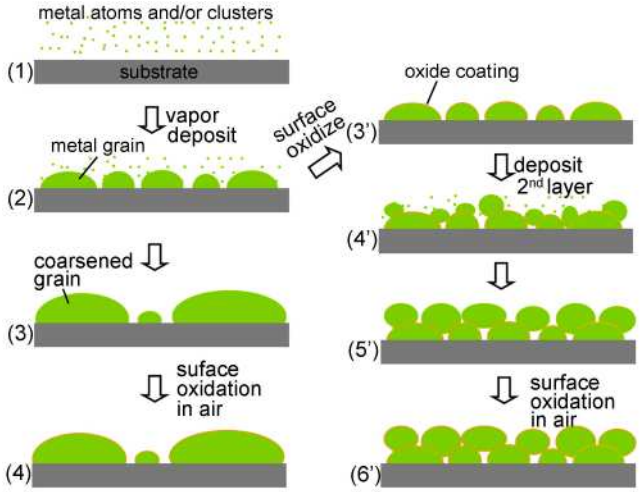

Fig. 2. Schematic illustration of the metallic films with the same nominal thickness prepared by routine method (route 1-2-3-4) and the refinement (route 1-2-3′-4’-5′-6’). The latter is composed of two layers of refined grains as a result of the interdiction of homoepitaxy caused by the oxide coating on the metal surface.

3.2 Transparency of the In, Sn, and metallic oxide films

The transparency of the Sn, In and corresponding oxide films should be discussed to clarify the applicable wavelength(s) and how the oxides affect transparency.

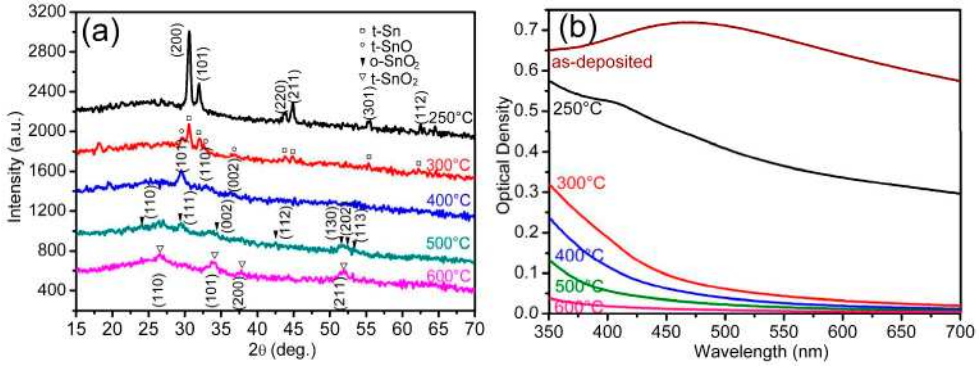

Fig. 3. (a) XRD spectra of 20 nm Sn films heated at different temperatures for 5 min, showing the phase evolution from Sn to SnO, orthorhombic (o-) SnO_2 and finally to tetragonal (t-) SnO_2. (b) NUV-vis spectra of the films annealed at different temperatures, the t-SnO_2 film has an OD less than 0.04 from 350 to 700 nm.

Figure 3(a) shows the phase evolution of the 20 nm Sn films heated at different temperatures for 5 min, and Fig. 3(b) shows the optical density (OD) spectra of the films from 350 to 700 nm. The phase evolution is similar to the reported result [11]. It is known from the spectra that the t-SnO_2 (sample annealed at 600 °C) is the most transparent, the OD value of the t-SnO_2 is below 0.04 (T > 91%) even at 350 nm. The t-SnO is the main phase of the sample annealed at 400 °C, it has an OD below 0.24 (T = 58%) from 350 to 700 nm. The as-deposited Sn is opaque and has an OD of 0.65 (T = 22%) at 350 nm. The distinction of the OD can be larger by using a thicker film. The results verify that the Sn and tin oxides system

#121143 - $15.00 USD Received 8 Dec 2009; revised 12 Jan 2010; accepted 12 Jan 2010; published 25 Jan 2010

is suitable for photolithography in the wavelength range from visible to NUV region down to 350 nm, covering some commonly used wavelengths such as I-line and G-line.

In the case of indium, there exists only one stable oxide, In_2O_3, with the body centered cubic (BCC) structure. The In-In_2O_3 system is simper than the Sn and tin oxides system. Figure 4 shows that the annealed In film (In_2O_3) is very transparent in the visible region. Although becomes less transparent with the decreasing of wavelength in NUV region, the optical density of the In_2O_3 film is still small. For example, a 20 nm In film can have a OD ranging from 1.10 to 0.10 (*T* from 7.7% to 79%) at 365 nm in an oxidation process, and the OD range of a 30 nm In is from 1.55 to 0.15 OD (*T* from 2.8% to 71%). The results are comparable to the HEBS glass which have an OD range of 0.2-1.2 at 365 nm when using a 15 kV accelerating voltage of the electron beam [12].

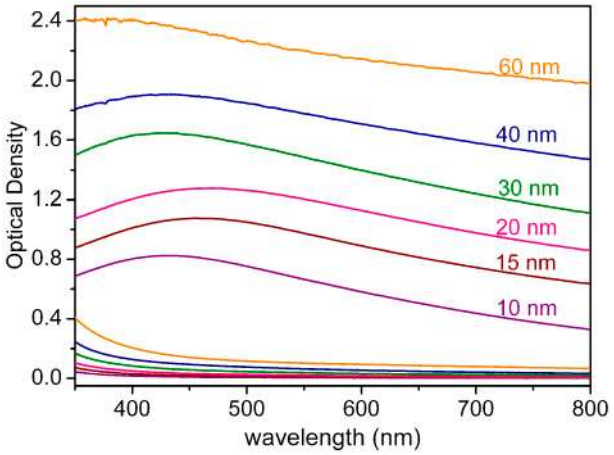

Fig. 4. NUV-vis spectra of In films with different thicknesses (upper part), and those of the films annealed at 350 °C for one hour (below). Spectra of an In film and the corresponding In_2O_3 film are in the same color.

3.3 Laser direct writing of MTMO grayscale masks

The grayscale masks were fabricated by using a laser beam. In the interaction of a laser beam with a metallic film, the absorption part of the laser's energy converts to heat, causing temperature rise and metal oxidation. The Sn and tin oxides system has been proved to have two kinds of distinct oxidation process by using short (< 1000 ns) and long (> 10000 ns) single pulse exposure. Under short laser pulse exposure, the surface layer of the Sn is oxidized and transformed to a transparent amorphous-SnO_x (a-SnO_x) coating [13]. Complicated components including Sn, SnO, orthorhombic (o-) SnO_2 and tetragonal (t-) SnO_2 are found under the long pulse exposure [14]. The distinct difference of transmittance between Sn and its oxides (include a-SnO_x), and the mixture nature of the film with the mixture ratio determined by laser power make the film's transmittance changeable. Therefore, by controlling the laser power, diverse grayscale patterns can be fabricated. Figure 5(a) show the transmitted grayscale images of a wolf fabricated in a refined Sn film with good gray levels and fine structures, while Fig. 5(b) was fabricated in a common Sn film with big grains and rough surface. It is obvious that the non-refined film is incapable for high-resolution grayscale lithography. The favorable results of the refinement can be regarded as a nanometer size effect: the ultrafine nano-grains have large specific surface ratio, so that the film is apt to be oxidized because of the large specific surface energy and short diffusion path of oxygen atoms.

The grayscale patterns can also be fabricated in the In films. Figure 6(a)-(c) shows a set of optical images with discrete and continuous gray levels. In the writing process the laser powers is below 15 mW and the pulse width is 1.0 μs (Fig. 6(a) and (c)) and 100 ns (Fig. 6(b)). The brighter areas are exposed by higher laser power. Complex patterns are shown in

#121143 - $15.00 USD Received 8 Dec 2009; revised 12 Jan 2010; accepted 12 Jan 2010; published 25 Jan 2010

Fig. 6(d) and (e), with a pulse width of 1.0 μs and 1.0 ms, respectively. Many dot defects are observed in the latter. Our experience tells us that the dot defects tend to appear only under the long time exposure, typically when the pulse width is longer than 20 μs. Therefore, these dot defects can be suppressed easily by using shorter pulses and higher powers.

The good gray levels and fine structures of grayscale patterns in both Sn and In films imply that the MTMO grayscale masks can be used for high-resolution grayscale lithography.

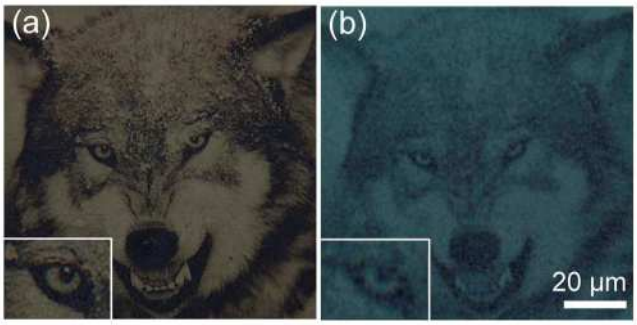

Fig. 5. (a) and (b) Grayscale patterns written in the refined and roughly surfaced 20 nm Sn films, respectively. The latter does not reveal fine structures of the wolf. The insets are magnified images of the wolf's eye, clearly showing that the refined film possess much better gray levels and finer features.

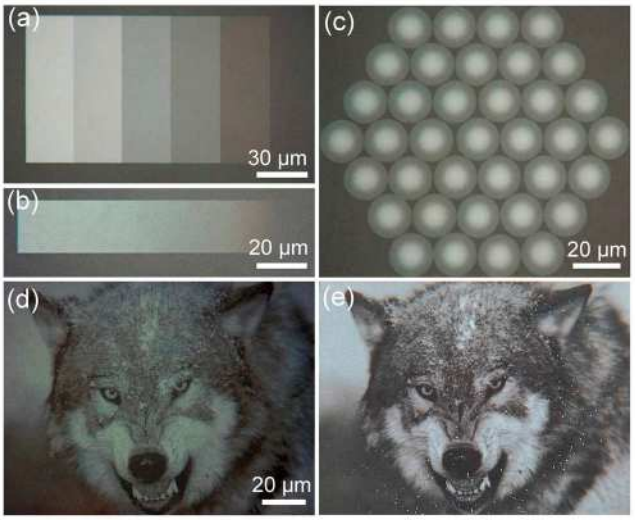

Fig. 6. (a)-(c) A set of grayscale pattern fabricated in a refined In film. (d) and (e) Complex grayscale patterns written under 2.5-10 mW 1.0 μs pulse exposure and 1.5-8 mW 1.0 ms pulse exposure, respectively. Image (e) is color-inverted.

3.4 Structure evolution of the MTMO grayscale masks

The Sn and tin oxides system has been proved to contain Sn and a-SnO_x under short pulse exposure or Sn, SnO, o-SnO_2 and t-SnO_2 under the long pulse exposure (see Fig. 7). An original Sn grain is decomposed into several subgrains, which may be in different structures thereby influence the transparency of the area.

In_2O_3 is used as the main component of the transparent conductive film ITO. It is also the sole stable oxide of In, therefore, the In-In_2O_3 system is much simpler than the Sn and tin oxides system.

Figure 8 shows the bright field TEM images of the as-deposited and laser exposed In films. The Moiré fringes in the film exposed at 0.9 mW symbolize the layered oxidation of

#121143 - $15.00 USD Received 8 Dec 2009; revised 12 Jan 2010; accepted 12 Jan 2010; published 25 Jan 2010

the metal, i.e., the film is an In_2O_3/In bilayer. At higher powers, e.g., 1.1 mW, the In film has almost been oxidized completely, thus the Moiré fringes are vanished. The results agree well with the SAED results shown in Fig. 9. The SAED patterns of an as-deposited In film and that exposed at various powers of 0.7, 0.9, 1.1 and 1.5 mW with laser pulse of 200 ns is shown in Fig. 9(a)-(e), the diffraction intensity of In decreases meanwhile that of In_2O_3 increases with the increasing of the laser power, and at 1.5 mW In has been fully transformed to In_2O_3. The

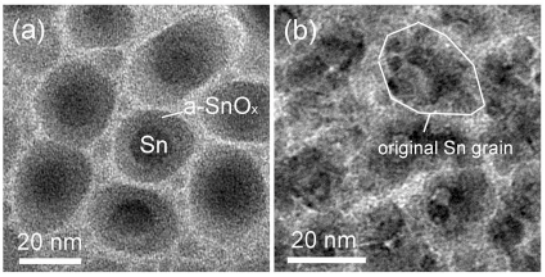

Fig. 7. TEM images of Sn films exposed under (a) 200 ns and (b) 1.0 ms pulse. There are several subgrains in the domain of an original Sn film and they may be in different structures.

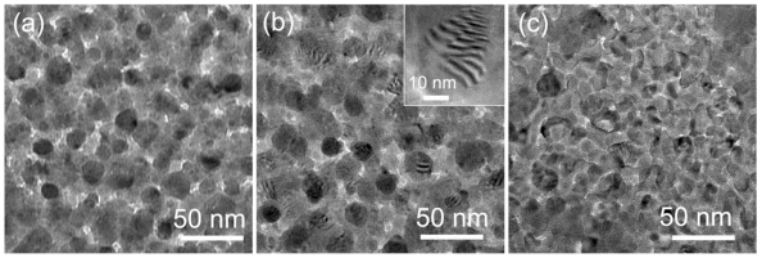

Fig. 8. Bright field images of (a) as-deposited 20 nm In film and laser exposed areas of the film with powers of (b) 0.9 mW and (c) 1.1 mW. Moiré fringes as a symbol of layered oxidation are found in (b). The inset in (b) is a magnified TEM image, showing the Moiré fringes.

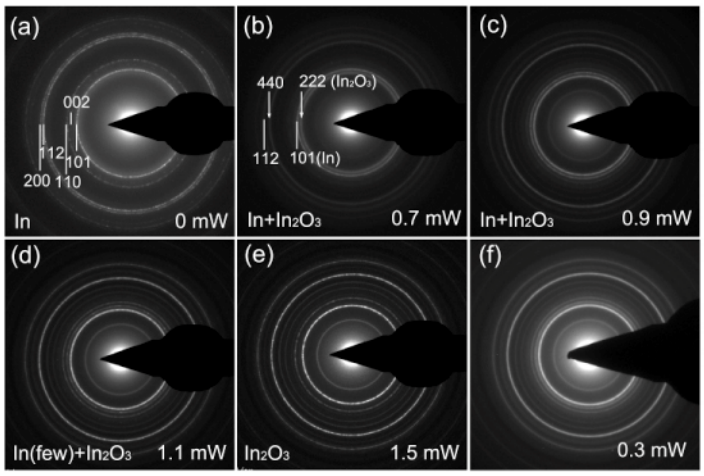

Fig. 9. (a)-(e) SAED patterns of 20 nm In films exposed at different laser power with the pulse width of 200 ns, showing the phase evolution from In to In_2O_3. (f) SAED pattern of an In film exposed at 0.3 mW, pulse width is 1.0 ms.

#121143 - $15.00 USD Received 8 Dec 2009; revised 12 Jan 2010; accepted 12 Jan 2010; published 25 Jan 2010

SAED patterns of 0.7, 0.9 and 1.1 mW all give two phases: In and In_2O_3, in other words, the film is a mixture, verifying the In_2O_3/In bilayer structure. The structure analysis demonstrates that the component formula (In_2O_3:In) can be controlled by simply tuning laser power so that the transparency is controllable as well. Apart from the power, pulse width of the laser beam affect the oxidation process as well. Figure 9(f) reveals the SAED pattern of a In_2O_3/In mixture exposed by 0.3 mW with 1.0 ms pulse, the In_2O_3:In ratio is estimated to be close to or higher than that in Fig. 9(c) exposed at 0.9 mW for 200 ns. It can be easily understood because long time exposure promotes the metal oxidation.

3.5 Mechanism of the grayscale features of the MTMO systems

The mechanism of the grayscale feature of the MTMO grayscale masks can be ascribed to the coexistence of the opaque metal and the corresponding transparent metallic oxide(s). However, details for the Sn-tin oxides and In-indium oxide systems are different.

Under the short pulse exposure (<1000 ns) of laser, the Sn grains are transformed to the a-SnO_x/Sn core/shell structures, the gray level is determined by the thickness of the transparent a-SnO_x. In this case, the LDW of Sn films can be regarded as the layered oxidation, shown in Fig. 10(a). This model is only suitable for relatively thin Sn films, typically no more than 20 nm. The minimum OD is not as small as that exposed under long pulse, for example, OD ranging from 0.73 to 0.20 for a 20 nm Sn film under 200 ns pulse, while the latter (1.0 ms pulse) can have a wide range from 0.73 to 0.08 [14].

When a Sn film is exposed in long pulse (>10000 ns), the Sn grains are decomposed to subgrains with a scale of ~ 5 nm. These subgrains can be in different structures, i.e., Sn, t-SnO, o-SnO_2 and t-SnO_2, and the t-SnO_2 is the most transparent among them. The gray levels of the Sn-SnO-SnO_2 system are determined by the mixture ratio of different phases. When completely transformed to t-SnO_2, OD of the film achieves its minimum. Schematic illustration of this model is shown in Fig. 10(b).

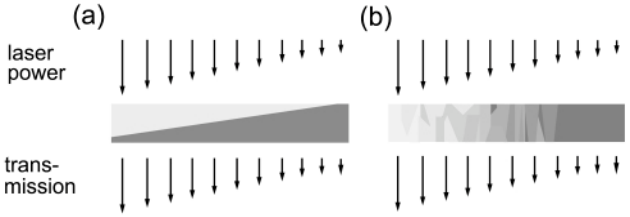

Fig. 10. Schematic illustration of (a) layered oxidation model and (b) grain model for explaining the grayscale features of MTMO systems. Layered oxidation model is suit for In and short pulse exposure of Sn (the Sn and a-SnO_x system) while grain model is suit for long pulse exposure of Sn (the Sn-SnO-SnO_2 system).

#121143 - $15.00 USD Received 8 Dec 2009; revised 12 Jan 2010; accepted 12 Jan 2010; published 25 Jan 2010

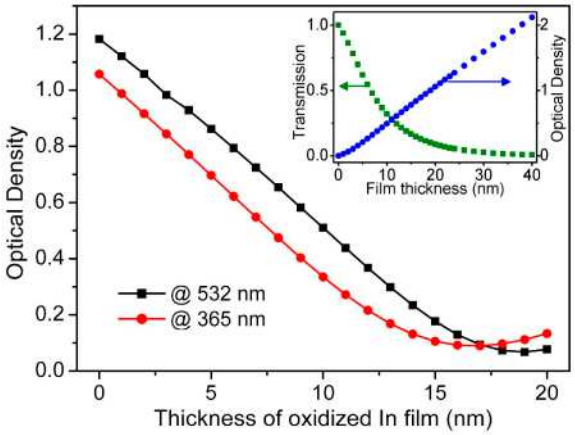

Fig. 11. Simulation of the In_2O_3/In bilayer's OD at wavelengths of 365 and 532 nm, showing that the film achieves the minimum OD before complete oxidation. In is 20 nm thick before being oxidized. The inset shows the OD or *T* of the In film versus film thickness.

Indium does not transform to amorphous oxide under short pulse exposure, In_2O_3 is its sole oxide. As has been clarified, the In film is layered oxidized as indicated from the Moiré fringes. Therefore, the OD values are determined by the thickness of the In_2O_3. The mechanism of the grayscale feature can be explained by the model shown in Fig. 10(a). Simulation of the OD of the In_2O_3/In bilayer (In film is 20 nm thick before oxidation) at wavelengths of 365 and 532 nm is shown in Fig. 11, from which we know the film's transmission achieves its maximum before being completely oxidized. This trend is especially remarkable at a short wavelength, at which In_2O_3 is less transparent. The explanation is simple: the OD of the In_2O_3 film is oscillated with the thickness (In fact, OD of In_2O_3 is decreased with the thickness in our experimental range) while that of the In is almost linear to the film thickness (see the inset in Fig. 11). When the film is oxidized, In is even more transparent than In_2O_3 when it is thinner than 4 nm, so that In_2O_3 contributes the majority of the film's OD. According to this result, the film does not need to be fully oxidized in laser writing.

Regardless the In or the Sn film, the gray level of the exposed area is a function of laser power, so that the LDW technique is adequate for making grayscale masks using In or Sn films. Our experiment shows LDW of a Sn/In alloy film does not lead to better results than a In or Sn film. From another perspective, the good electric transport of the oxides of the Sn/In alloy, the ITO, is not what we search for.

3.6 Comparison of Sn and In films used as grayscale masks

The low melting point metals In and Sn having very transparent and stable oxide, that's why we choose them as the media for fabricating grayscale mask. Characteristics of the two films, however, are not exactly the same. Here we compare the two grayscale masks on OD range, energy consumption in mask fabrication and their stability.

(1) In has a larger OD than Sn with the same thickness. For example, a 20 nm In has an OD of ~ 1.1 while the latter has an OD of only 0.65. Generally speaking, we need a larger OD range in the MTMO grayscale mask. Although adding film thickness results in a larger OD of a metal, it also causes a increase of oxide's OD, when the oxide's thickness is below $0.25\lambda/n$, where λ is the wavelength of light, n is the refractive index of the oxide. For a SnO_2 or In_2O_3 film under I-line illumination, it achieves its minimum transmittance at a thickness of around 45 nm, and the corresponding thickness of metal film is about 35 nm. Moreover, the metallic film is hard to be fully oxidized when it is thicker than 40 nm. Therefore, In is preferred, although SnO_2 is slightly more transparent than In_2O_3.

(2) The Sn and a-SnO_x system is not a very good candidate using as a grayscale mask because this system can be well controlled only when the film is thin (< 20 nm), moreover,

#121143 - $15.00 USD Received 8 Dec 2009; revised 12 Jan 2010; accepted 12 Jan 2010; published 25 Jan 2010

the a-SnO_x is not as transparent as SnO_2 or In_2O_3. Therefore, we have to use the long pulse exposure (> 10 μs) to prepare the Sn-SnO-SnO_2 system. The long pulse exposure, however, implies high energy consumption and long writing time. Typically, the writing need a laser dose of 15-4000 J·cm^{-2}. The In-In_2O_3 system can be obtained by using short pulse exposure. The pulse width can be 100 ns (corresponding energy density lower than 1.5 J·cm^{-2}) or even shorter, so that energy consumption is lower. The difference of the pulse width needed for the two MTMO systems may be originated from that the formation of t-SnO_2 needs intermediate oxides, while In_2O_3 is directly transformed from In. The results demonstrate that the grayscale mask based on In-In_2O_3 system is more energy-saving.

(3) With respect to the stability of the two MTMO systems, the oxides involved in our study are all stable in the form of thin film, and the metallic Sn grain is coated by a very thin a-SnO_x layer, while In has a thin In_2O_3 layer formed in air to prevent further oxidation, therefore they are stable. Although SAED measurement reveals the existence of a spot of In_2O_3 in unexposed areas of In film after exposure in air, OD of the film is almost unchanged because the oxide layer is rather thin. In addition, we have reported that after several-hour-heating at 100 °C no change is observed in a Sn film [14], while In film gets slightly more transparent (can hardly be detected by naked eyes), and this change can be avoided by using a protective layer. Our experimental results show both grayscale masks are stable (graylevels are not changed) after long time exposure in air ambience or UV light, demonstrating that the MTMO masks are competent for ordinary gray-tone lithography in laboratory. A thin SiO_2 protective layer deposited on the mask can significantly enhance its stability in more rigorous conditions. The stability of MTMO grayscale masks needs to be studied further if they are to be used in industry.

3.7 Applications of the M-MTO grayscale masks

The grayscale mask is typically used for the fabrication of 3D microstructures. We have made various 3D microstructures with smooth surface by using the MTMO grayscale masks, as shown in Fig. 12(a) and (b). Focusing effect of the microlens array is shown in Fig. 12(c). Besides, the MTMO systems can also be used as amplitude gratings or other micro-optics with variable amplitude (Fig. 12(d)).

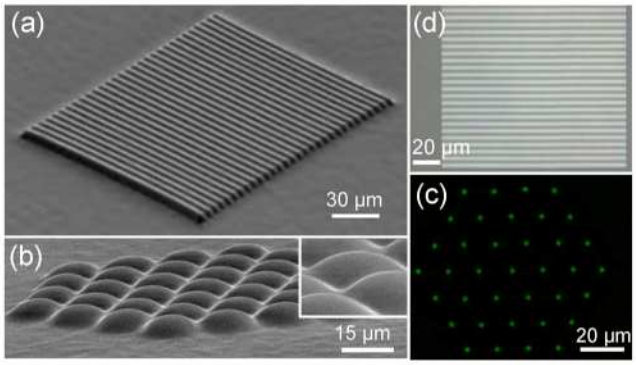

Fig. 12. SEM images of (a) surface relief phase grating with a period of 5 μm and (b) microlens array fabricated in a SU-8 film by using MTMO grayscale masks. The inset in (b) shows that the surface of the lenses is very smooth. (c) Focusing effect of the microlens array. (d) Optical image of a MTMO grayscale pattern, which can be used as an amplitude grating or a mask for fabricating surface relief grating.

4. Conclusion

We have developed a new class of grayscale photomasks based on the metal-transparent-metallic-oxides systems and studied the fabrication, mechanism and applications of the masks in detail. The masks are fabricated in only two simple steps: film deposition and laser writing. The masks are suitable for grayscale lithography in the NUV-vis region at least down to 350

#121143 - $15.00 USD Received 8 Dec 2009; revised 12 Jan 2010; accepted 12 Jan 2010; published 25 Jan 2010

nm. The grayscale mask based on the In film presents advantages for having larger OD range and lower energy consumption than the Sn film. 3D microstructures are successfully obtained using the MTMO grayscale masks. Technologically, the MTMO grayscale masks can be obtained easily with a laser writer in air ambience so that our technique provides a cost-effective approach for the fabrication of grayscale masks and 3D microstructures.

In this paper, we have discussed the theory and preparation of ultrafine grained metallic films those are qualified for the study, as well as the mechanism and two models of the MTMO grayscale masks. Performances such as resolution, cost, writing repeatability, effect of film thickness and contour accuracy of microstructures in lithography are also very important for a grayscale mask and will be further discussed in another work.

Acknowledgement

This work was supported by the funds of NSFC (90606025, 10974037), the KIP of CAS (KJCX2-YW-M06) and NBRPC (2006CB932603, 2010CB934102).

#121143 - $15.00 USD Received 8 Dec 2009; revised 12 Jan 2010; accepted 12 Jan 2010; published 25 Jan 2010